

UC Irvine

UC Irvine Previously Published Works

Title

Increasing the Stability of Recombinant Human Green Cone Pigment.

Permalink

<https://escholarship.org/uc/item/2cd8s0w4>

Journal

Biochemistry, 57(6)

Authors

Owen, Timothy

Salom, David

Sun, Wenyu

et al.

Publication Date

2018-02-13

DOI

10.1021/acs.biochem.7b01118

Peer reviewed



Published in final edited form as:

Biochemistry. 2018 February 13; 57(6): 1022–1030. doi:10.1021/acs.biochem.7b01118.

Increasing the Stability of Recombinant Human Green Cone Pigment

Timothy S. Owen[¶], David Salom[¶], Wenyu Sun[§], and Krzysztof Palczewski^{¶,*} 

[¶]Department of Pharmacology, Cleveland Center for Membrane and Structural Biology, School of Medicine, Case Western Reserve University, 2109 Adelbert Road, Cleveland, Ohio 44106, United States


[§]Polgenix, Inc., Cleveland, Ohio 44106, United States

Abstract

Three types of cone cells exist in the human retina, each containing a different pigment responsible for the initial step of phototransduction. These pigments are distinguished by their specific absorbance maxima: 425 nm (blue), 530 nm (green), and 560 nm (red). Each pigment contains a common chromophore, 11-*cis*-retinal covalently bound to an opsin protein via a Schiff base. The 11-*cis*-retinal protonated Schiff base has an absorbance maxima at 440 nm in methanol. Unfortunately, the chemistry that allows the same chromophore to interact with different opsin proteins to tune the absorbance of the resulting pigments to distinct λ_{\max} values is poorly understood. Rhodopsin is the only pigment with a native structure determined at high resolution. Homology models for cone pigments have been generated, but experimentally determined structures are needed for a precise understanding of spectral tuning. The principal obstacle to solving the structures of cone pigments has been their innate instability in recombinant constructs. By inserting five different thermostabilizing proteins (BRIL, T4L, PGS, RUB, and FLAV) into the recombinant green opsin sequence, constructs were created that were up to 9-fold more stable than WT. Using cellular retinaldehyde-binding protein (CRALBP), we developed a quick means of assessing the stability of the green pigment. CRALBP testing also confirmed an additional 48-fold increase in pigment stability when varying the detergent used. These results suggest an efficient protocol for routine purification and stabilization of cone pigments that could be used for high-resolution determination of their structures, as well as for other studies.

Graphical abstract

* **Corresponding Author.** Address: Department of Pharmacology, School of Medicine, Case Western Reserve University, 10900 Euclid Ave, Cleveland, OH 44106–4965, USA. Tel.: 216-368-4631. Fax: 216-368-1300. kxp65@case.edu.

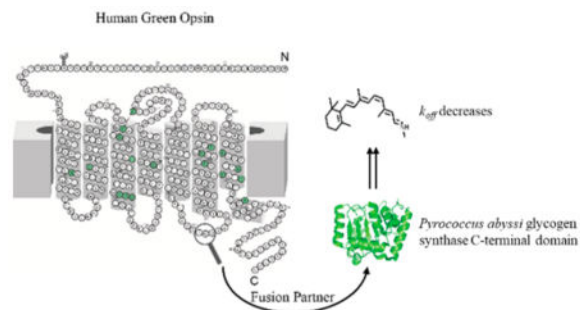
ORCID 

Krzysztof Palczewski: 0000-0002-0788-545X

Author Contributions

T.S.O., D.S., W.S., and K.P. participated in research design. T.S.O., D.S., and W.S. conducted experiments. T.S.O., D.S., and W.S. contributed new reagents or analytical tools. T.S.O., D.S., W.S., and K.P. performed data analysis.

The authors declare the following competing financial interest(s): K.P. is the Chief Scientific Officer of Polgenix, Inc.



INTRODUCTION

Vertebrate retinas have two morphologically distinct types of ciliated photoreceptor cells—rods and cones^{1,2}—with highly membranous distal structures called outer segments. The visual pigment rhodopsin (Rho) resides in the rod outer segments,^{3,4} whereas three genetically distinct pigments are located in the cone outer segments.⁵ Based on the type of opsin expressed in a cone cell, these can be further divided into “short” (blue), “medium” (green), and “long” (red) wavelength types with absorbance maxima in humans of 425, 530, and 560 nm, respectively.⁶ In addition to the visual pigments, outer segments contain all of the components of the phototransduction cascade needed for light signal amplification and quenching^{7,8}

Rhodopsin shares 41%, 38%, and 37% sequence identity with blue, green, and red cone pigments, respectively.^{5,9} Green and red pigments share almost 96% sequence identity, whereas green and blue pigments share ~70% sequence identity. All these pigments possess a common chromophore: 11-*cis*-retinal. 11-*cis* retinal is linked to the green pigment by a protonated Schiff base (PSB) of which the environment has been examined by Raman spectroscopy.¹⁰ In green cone pigment, Glu129 stabilizes the PSB, that would otherwise be unstable in a hydrophobic environment.¹¹ Determination of the bovine rhodopsin structure in the year 2000 marked the first three-dimensional (3D) map of any GPCR.¹² Since then, the structural understanding of cone pigments has been based solely on homology modeling with Rho.⁹ Unfortunately, the resolution of such models cannot answer key questions about cone-mediated vision. Critically, the question of how amino acid residues at varying distances from the chromophore modulate the spectral properties of the different cone pigments remains unanswered. In various model systems, different molecular environments within the chromophore-binding pocket can markedly change the maximum absorption over a 250 nm range. Spectral tuning of the cone pigments will likely depend on the distance of the chromophore from the opsin counterion, critical amino acid residues, water molecules in the transmembrane portion of the receptor, the presence of anions and cations, and the conformation of the chromophore.¹³ These features can only be resolved if accurate atomic scale structures are obtained. Unfortunately, the lack of an abundant natural source of cone pigments and the inherent instability of recombinant cone pigments have hindered their crystallization. Instability of the green pigment in particular is reflected by its significant difference in melting temperature, compared to bovine Rho,¹⁴ and previous efforts to characterize green pigment also have been compromised by its dark release of 11-*cis* retinal.

Figure 1 shows a two-dimensional (2D) model of Rho and human green cone opsin.

Recent advances in the structural determination of several GPCRs by using thermostable fusion constructs¹⁵ may provide a strategy for determining the structures of cone pigments. Thermo-stabilizing proteins successfully used for structural determinations include Cytochrome *b*₅₆₂RIL (BRIL),^{15,16} T4 lysozyme (T4L),^{17,18} the *Pyrococcus abyssi* glycogen synthase C-terminal domain (PGS),¹⁹ rubredoxin (RUB),¹⁵ and flavodoxin (FLAV)¹⁵ (Figure 1C). Here, we describe the expression and characterization of human green cone pigment fused through intracellular loop 3 (ICL3) to these five different thermostabilizing proteins. ICL3 have been found to have variable lengths and pronounced structural flexibility in many GPCRs that has been shown by its high proteolytic susceptibility and high hydrogen–deuterium exchange rate.²⁰ When the native sequence is left in a construct sequence, it is often found disordered in crystallized GPCRs.^{12,21} Expression of these fusion proteins demonstrated a 9-fold increase in the thermostability of recombinant human green cone pigment. Addition of the fusion partner did not cause a shift in the absorbance of 11-*cis*-retinal, indicating that the protein retained its native conformation. Using a new assay based on CRALBP, a relatively new class of detergents, maltose neopentyl glycol (MNG) amphiphiles, led to a further 48-fold increase when varying the detergent used for solubilization and purification. These advances in the purification and stabilization of cone pigments will enable high-resolution determination of their structures to better understand the basis for spectral tuning underlying color perception.

MATERIALS AND METHODS

Materials

Except as noted below, chemical reagents were purchased from Sigma–Aldrich (St. Louis, MO) in the highest purity available. LB media was purchased from USB (Cleveland, OH). Water from a Milli-Q purification system (resistivity = 18.2 mΩ cm) (ED Millipore, Billerica, MA) was used to prepare all reagents and buffer solutions. PBS buffer was composed of 10 mM dibasic sodium phosphate, 1.8 mM monobasic potassium phosphate, 2.7 mM potassium chloride, and 137 mM sodium chloride at pH 7.2. Green opsin constructs DNA to were purchased and synthesized by Genscript (Piscataway, NJ) with the designing that has the five different partners inserted in the position of IL3 of green opsin. All constructs DNA were synthesized with a replacement of the native C-terminus with the 1D4 epitope TETSQVAPA.

Generation of Recombinant Baculovirus and Optimization of Cell Culture Expression

All constructs were cloned into pFastBac HTa from a Bac-to-Bac Vector Kit (Thermo Scientific, Waltham, MA). Bacmid was produced using the Bac-to-Bac Baculovirus Expression System protocol by Invitrogen (Carlsbad, CA). Initial transfection of Sf9 cells was done by adding 1 μg of bacmid DNA to cells in log-phase growth that became attached in a six-well plate. After 5 days, the supernatant was harvested and 1.5 mL of P1 virus was added to 40 mL of cells at a density of 1.5×10^6 cells/mL. After 4 days, the P2 virus was harvested by centrifuging the culture at 2500g for 5 min. The P3 virus stock was prepared by adding 2 mL of P2 virus to 800 mL of Sf9 cells at a density of 2×10^6 cells/mL. The

expression of each construct was tested using a viral titration method, with different amounts of P3 stage virus used to infect the same quantity of Sf9 cells. Following a three-day incubation, the P3 virus was harvested in the same fashion as the P2 virus and then used to optimize expression. Virus amounts were doubled sequentially, compared to each previous sample. All samples were harvested on day 2, subjected to sodium dodecyl sulfate polyacrylamide gel electrophoresis (SDS-PAGE) and later transferred to a polyvinylidene fluoride (PVDF) membrane for detection with 1D4 antibody.

Regeneration and Purification of Green Opsin Constructs

All subsequent purification steps were performed either at 4 °C or on ice in a dark room under dim red light. To isolate membranes, frozen Sf9 cells were first thawed and disrupted in a Dounce homogenizer and a hypotonic buffer composed of 25 mM HEPES, pH 7.0, plus protease inhibitors (10 µg/mL benzamidine, 1 mM PMSF). Membranes then were pelleted by centrifugation at 50 000g for 50 min. Membrane homogenization in the same hypotonic buffer and centrifugation were repeated once, followed by two or three washes with a hypertonic buffer (50 mM HEPES, pH 7.0, 1 M NaCl, 1 mM MgCl₂, benzonase nuclease, plus protease inhibitors). Washed membranes were resuspended in buffer, incubated 30 min with 11-*cis*-retinal and then detergent was added to achieve final concentrations of 50 mM HEPES, pH 7.0, 0.25 M NaCl, 30 µM 11-*cis*-retinal, 15 mM *n*-dodecyl β-D-maltoside (DDM) or 3.6 mM lauryl maltose neopentyl glycol (LMNG) and benzonase and protease inhibitors, in a final volume of 42 mL. The suspension was rotated for 3 h, and insoluble material was removed by centrifugation at 50 000g for 50 min. An aliquot of each supernatant was analyzed by SDS-PAGE, followed by immunoblotting with alkaline phosphatase-coupled 1D4 antibody for detection of the green opsin constructs.

Pigments were purified from supernatants by immunoaffinity chromatography with an anti-rhodopsin C-terminus 1D4 antibody. A quantity of 2 mL of 1D4-Sepharose beads was added to the supernatants and incubated for 2 h at 4 °C with slow rotation. The resin then was transferred to a column and washed with 15 mL of buffer consisting of 50 mM HEPES, pH 7.0, 150 mM NaCl, and 1 mM DDM (or 0.2 mM LMNG). Pigments were eluted overnight on batch by adding to the 1D4-Sepharose beads 1.5 mL of buffer consisting of 200 mM HEPES, pH 7.0, 0.1 M NaCl, and 1 mM DDM (or 0.2 mM LMNG), supplemented with 0.8 mg/mL of competing TETSQVAPA peptide. Ultraviolet–visible (UV-Vis) absorption spectra of the purified pigments were recorded, and then each sample was analyzed by electrophoresis on a 4%–12% acrylamide, SDS-polyacrylamide gel with MOPS used as the running buffer. For visualization, gels were stained with either Coomassie blue or silver stain.

UV–Vis Wavelength Spectroscopy and Analysis of Stability by Thermal Bleaching

UV–Vis spectroscopy was conducted with a Cary 50 Bio UV-Vis spectrophotometer at a regulated constant temperature of 30 °C. Thermostability of the green opsin constructs was measured on the same day that eluates were collected over a 4 h period. Following measurements of spectra over time, samples were bleached with light at 530 nm and their spectra were acquired again. Absorption at 530 nm was then plotted against time and a pseudo-first-order decay rate constant was calculated with a set minimum at 530 nm

determined from the bleached sample. Pseudo-first-order rate constants (k_{obs}) for each construct were calculated as follows:

$$\text{pigment}_{\text{time}} = Ae^{-k_{\text{obs}}t} + C$$

with best fit values for A and k_{obs} obtained by nonlinear regression using Excel solver, and C is set by the bleached construct spectral absorbance at 530 nm. The apparent half-life for each construct was calculated by the apparent k_{obs} for each construct as follows:

$$t_{1/2} = \frac{0.693}{k_{\text{obs}}}$$

CRALBP Competition Assay

CRALBP was expressed in BL21(DE3) *E. coli* as described in Crabb et al.²² Following induction at 0.6 O.D. with 1 mM IPTG, the culture was incubated overnight at 20 °C before harvesting. Cultures were centrifuged at 6000g and then resuspended in lysis buffer. Lysis buffer was composed of 50 mM sodium phosphate, 250 mM NaCl, 100 mM KCl, 5% glycerol, and 0.1% Triton X100 at pH 7.1. The suspension then was sonicated on ice at intervals over 5 min with 30 pulses, each followed by a 30-s rest period. Lysozyme was then added to a final concentration of 100 µg/mL and benzonase to achieve 20 µg/mL. This suspension was incubated for 20 min at 4 °C with gentle rocking before being centrifuged at 10 000g for 15 min. Finally, the protein in the supernatant was further purified by ion affinity chromatography using the Ni-Sepharose 6 Fast Flow (GE Healthcare, Little Chalfont, U.K.) protocol for binding, washing, and elution of His-tagged CRALBP. Elution fractions were dialyzed against PBS to remove imidazole, followed by concentration for subsequent use in a CRALBP competition assay. The CRALBP competition assay was developed to determine the enhanced affinity of 11-*cis* retinal for opsin with CRALBP as the competitor. Regenerated WT-green opsin (0.6 µM final) in 1 mM DDM was incubated with various salts (0.5 M final) or detergents (0.5 mM final) for 30 min at 4 °C. Following incubation, CRALBP was added to a final concentration of 4 µM and incubated for another 30 min at 4 °C. The mixture was then centrifuged at 45 000g for 10 min at 4 °C and spectra were recorded from the clarified mixture.

RESULTS

The crystallization of cone pigments for high-resolution determination requires improvements in the expression, purification, and stabilization of recombinant constructs. Atomic resolution studies of such pigments then will provide valuable information about the primary mechanisms underlying their spectral tuning and color perception.

Expression and Purification of Recombinant Human Green Cone Pigment

Figure 2 illustrates the titration of P3 virus for each opsin construct with a known quantity of Sf9 cells and the associated expression measured by visualizing the quantities of pigment protein on immunoblots stained with 1D4 antibody specific for the opsin C-terminus. The

optimal amount of virus was obtained with a 1:50 dilution of P3 virus to Sf9 cells at a density of 3.2×10^6 . These conditions were used for all subsequent expressions. Rho has been shown in the literature to form higher-order oligomers at high expression levels, as well as electrophoresis conditions, such as boiling the sample beforehand.^{23,24} Based on the expression in Figure 2, it appears that green opsin also forms oligomers as expression levels increase. Also, there is an apparent inconsistency with the expected molecular weight of the fusion constructs and the apparent molecular weights. It is common for GPCRs to run “faster” during electrophoresis due to the samples not being boiled to prevent aggregation and, therefore, not fully linearizing the peptide.

Using optimal expression conditions, we purified the constructs to analyze how the insertion partner would affect chromophore absorption following regeneration. Cell cultures were harvested after 3 days, and the cone opsin constructs were regenerated with 11-*cis* retinal and purified by 1D4 immunoaffinity chromatography. Figures 3A and 3B show the purified products of the six constructs from solubilized membranes in DDM and LMNG, as examined by 1D4 immunoblotting. The purity of the products solubilized in DDM was examined by SDS-PAGE and Coomassie staining (Figure 3C). Coomassie staining revealed that the only protein bands visualized were the 1D4 tagged constructs, which indicates their high degree of purity. To confirm that the insertion does not cause the aggregation of opsin, the PGS-opsin fusion was subjected to Superdex 200 size-exclusion chromatography, which revealed that the fusion protein exists mainly in a single, monodispersed state (Figure 3D). The other green opsin constructs yielded similar size-exclusion profiles.

Visual pigments are post-translationally modified, so this aspect of expressing the different constructs was addressed. Rho has two glycosylation sites in the N-terminal region (Figure 1), whereas the sequence of green pigment protein indicates only one site for glycosylation. Figure 4 shows the purified recombinant constructs including WT-green opsin visualized after SDS-PAGE and silver staining (Figure 4A). The same protein pretreated with PNGase-F to deglycosylate *N*-linked glycoproteins is shown (Figure 4B). Following treatment with PNGase-F, the pigments appear to undergo a mass shift of 2–3 kDa, consistent with the deglycosylation of a single site.

Examining the Chromophore: Absorption and Thermal Stability of the Fusion Constructs

Immediately following purification of the different fusion constructs, their spectra were determined (Figure 5). Each construct had an absorbance maximum of 530 nm in both DDM and LMNG. This coincides with the wild-type pigment absorption maximum indicating that the different constructs are correctly folded, their active sites are maintained, and the ICL3 insertions do not disturb chromophore binding. The FLAV fusion adds a secondary absorption peak, whereby the 11-*cis*-retinal peak appears broadened. This corresponds to the absorption maximum of the FLAV oxidized flavin mononucleotide group, which has a peak between 445 nm and 465 nm.²⁵ The yield for immuno-purification of the T4L construct was 0.4–0.8 mg of protein per liter of Sf9 cell culture. Inclusion of an additional purification step (gel filtration) resulted in a final yield of 0.28–0.56 mg per liter of Sf9 cell culture. For the rest of the constructs, typical immuno-purification yields are 0.5–1.0 mg/L for the BRIL, RUB and FLAV constructs, 0.9–1.8 mg/L for PGS, 0.6–1.2 mg/L for FLAV, and 0.07–0.14

mg/L for G1. These yields, except for G1, are appropriate for structural studies such as crystallization.

These purified products of the fusion constructs then were used to measure the thermostability of the pigments by examining the dissociation of 11-*cis*-retinal from their active sites. Thermal dissociation at 30 °C was monitored by measuring the change in absorbance of 11-*cis*-retinal bound in the active site versus free retinal which undergoes an absorbance shift from 530 nm to 385 nm. Figure 6A shows the time course of retinal dissociation for the PGS fusion construct in DDM. The decay of the 530 nm peak from each construct then was used to determine a rate constant, which, in turn, was used to calculate a half-life for that construct in DDM and LMNG (Figure 6B). The half-life values determined for each of the different constructs indicate that PGS provided the greatest resistance to thermal bleaching for the cone pigment, compared to WT in DDM. LMNG also provided higher resistance to thermal bleaching, which demonstrates the value of MNG detergents in purifying GPCRs and maintaining them in their active forms.

Competitive Retinal Binding Assay

Preventing chromophore dissociation from the regenerated pigment is critical for maintaining its stability and achieving crystallization. Thus, a quick and efficient method of determining pigment stability is needed to determine the conditions appropriate for crystallization. CRALBP is a 36-kDa water-soluble protein with two conformational states facilitating the intracellular transport of hydrophobic 11-*cis* retinoids.²⁶ CRALBP has a K_d value for 11-*cis* retinal of ~21 nM.^{22,27} Since the binding of CRALBP to retinal is very tight, it has the potential to act as a competitor of the chromophore bound in the regenerated pigment. After mixing the purified WT pigment in DDM with CRALBP, the chromophore peak at 530 nm completely disappeared (Figure 7A). However, if the WT pigment was incubated with LMNG or Cymal-6 before the addition of CRALBP, the chromophore peak at 530 nm was preserved. As shown above, the WT pigment has a higher stability in LMNG, compared to DDM, as seen by its greater degree of resistance to thermal bleaching (Figure 7A and 7B). Cymal-6 was chosen as a detergent derivative to test for stabilization in the presence of CRALBP, because it is widely used in solubilizing and crystallizing membrane proteins. The hydrophobic portion of Cymal-6, compared to DDM, has a terminal cyclohexane ring instead of a linear 11-carbon alkyl chain. Also, CMC values for DDM, Cymal-6, and LMNG are 0.17, 0.56, and 0.01 mM, respectively. As the CMC varies ~50-fold between Cymal-6 and LMNG, it seems to be apparent that the stability of the opsin is not dependent on the CMC but rather on the variation of the hydrophobic region of the detergent. Further analysis showed that the pigment without additive precipitated from solution, as evidenced by the disappearance of the corresponding band in the soluble fraction analyzed by SDS-PAGE and 1D4-immunoblotting (Figure 7B). However, when LMNG or Cymal-6 was added to the sample before incubation with CRALBP, the corresponding WT-pigment band was preserved (Figure 7B), which correlates with the preservation of the 530 nm chromophore peak (Figure 7A).

DISCUSSION

11-*cis* Retinal is the common chromophore for all eukaryotic visual pigments. “Spectral tuning” is the term used to describe how the absorption spectrum of this common chromophore is modulated when covalently attached to similar protein moieties of opsin to form the wide range of light-absorbing eukaryotic visual pigments. Structural information is needed to determine the role of specific amino acid residues, embedded water molecules in the transmembrane portion of the receptor, and other factors that underlie spectral tuning. Several studies have described the expression of recombinant human visual pigments but all efforts to crystallize them were impeded by their apparent instability. In this study, several approaches to enhance the stability of regenerated cone pigments were assessed, including the use of thermostabilizing proteins inserted into ICL3 and detergents other than DDM. Moreover, a fast screening method was developed to determine pigment stability by competition for binding with CRALBP.

Fusion Green Pigment Can Be Expressed and Purified in an Active Form from Insect Cells

A sufficient source of green cone pigment with close homology to the human pigment is not available from retinal tissue. This contrasts with Rho, which can easily be extracted from bovine retina.²⁸ Therefore, a different method is required to produce sufficient quantities of green cone pigment for biochemical characterization and potential structural analyses. Sf9 insect cells are being used increasingly more often to express recombinant human proteins, because of their ability to produce large quantities of post-translationally modified eukaryotic proteins in a short period.²⁹ Here, using a commercially available baculovirus system, the expression of WT human green cone pigment was optimized as well as that of human green cone pigment fused to five different thermostabilizing small proteins. To date, the insertion of T4L embodies the most successful approach enabling the crystallization of GPCRs, including the β_2 AR,³⁰ A_{2A}AR,³¹ dopamine D3 receptor,³² and chemokine CXCR4 receptor³³ among others. However, all five thermostabilizing proteins tested in this study have the potential to enhance stability and assist in crystal formation for structural determinations.³⁴

Here, the expression of human green pigment fused to each of the five small stabilizing proteins not only led to an increase in stability but also a higher yield of the modified proteins, compared to WT protein. Purified constructs run on SDS-PAGE exhibit a decrease in apparent mass, compared to the expected mass consistent with previous studies into GPCRs.³⁵ Comparisons of the purified pigments obtained from the different fusion constructs demonstrated that PGS provided the greatest recovery of membrane-regenerated pigment, followed by RUB, FLAV, BRIL, and T4L (see Figures 3 and 4).

Importantly, insertion of a thermostabilizing protein into ICL3 did not adversely affect the active site of the pigment, as the fusion proteins had the same chromophore absorbance at 530 nm as WT protein (Figure 5). This finding should be of interest to those attempting to crystallize other eukaryotic GPCRs.

Insertion of a Thermostabilizing Protein Decreases the Rate of Chromophore Dissociation

The green cone opsin fusion constructs also enhanced the stability of the pigment by slowing the thermal release of 11-*cis* retinal from the active site. PGS was especially effective and might be especially relevant to structural studies, since its insertion increased the protein's stability 9-fold in DDM and 2.6-fold in LMNG (Figure 6B). LMNG and other MNG derivatives have been shown to increase the thermostability of β_2 AR and other membrane proteins.³⁶ The MNG class of detergents also solubilize integral membrane proteins in their active conformations at lower concentrations than conventional detergents such as DDM.³⁶ In this study, we showed that LMNG not only helps the green pigment constructs resist thermal bleaching (Figure 6) but also allows for greater yields of purified protein (Figure 5B).

CRALBP Provides a Rapid Means of Determining Pigment Stability

Standard methods to determine the release of 11-*cis* retinal from the pigment active site are not satisfactory for rapid screening of potential small molecule stabilizers of human green pigment. Therefore, an improved screening method employing CRALBP was developed in this study to search for stabilizing reagents and to validate enhanced pigment stability found in LMNG. Following incubation of CRALBP with WT green pigment purified in DDM, the least-stable construct judging from its apparent chromophore dissociation half-life (Figure 6B), the chromophore peak at 530 nm completely disappeared, and this was accompanied by protein precipitation from solution (Figures 7A and 7B). These observations confirm previous results, indicating that opsin becomes unstable following chromophore dissociation.³⁷ When either LMNG or Cymal-6 was added, each prevented chromophore dissociation, preserving the 530 nm peak and maintaining the solubility of the pigment (see Figures 7A and B).

In summary, we describe the optimization of Sf9 cell-based expression of five human green cone opsin constructs fused to thermostable proteins in ICL3. These thermostabilized constructs can be regenerated with 11-*cis* retinal and can be purified by 1D4-immuno chromatography. Insertion of a thermostable protein into ICL3 did not affect the active site of the opsin, which retained its absorbance maximum at 530 nm, and it also induced a 9-fold increase in stability by preventing the dark release of the chromophore. Lastly, CRALBP can be used as a competitor for retinal binding to quickly characterize conditions that can stabilize the human green cone pigment for structural determinations. Here, the CRALBP assay successfully identified detergents capable of a 48-fold increase in pigment stability. Considered together, findings from this study demonstrate successful approaches for the expression, purification, and stabilization of human green cone pigment for further structural determinations to better understand the basis for spectral tuning.

Acknowledgments

Funding

This research was supported in part by grants from the National Institutes of Health (NIH) (Nos. EY009339, EY027283 and EY024864) to K.P. K.P. is the John H. Hord Professor of Pharmacology.

We thank Dr. Leslie T. Webster, Jr. and members of the Palczewski Laboratory for helpful comments on this manuscript.

ABBREVIATIONS

BRIL	cytochrome b562RIL
CMC	critical micelle concentration
COS	cone outer segment(s)
CRALBP	cellular retinaldehyde-binding protein
DDM	<i>n</i> -dodecyl β -D-maltoside
FLAV	flavodoxin
ICL3	intracellular loop 3
LMNG	lauryl maltose neopentyl glycol
MNG	maltose neopentyl glycol
PGS	<i>Pyrococcus abyssi</i> glycogen synthase C-terminal domain
PSB	protonated Schiff base
Rho	rhodopsin
ROS	rod outer segment(s)
RPE	retinal pigmented epithelium
RUB	rubredoxin
T4L	T4 lysozyme
WT	wild type

References

1. Kefalov VJ. Rod and Cone Visual Pigments and Phototransduction through Pharmacological, Genetic, and Physiological Approaches. *J. Biol. Chem.* 2012; 287:1635–1641. [PubMed: 22074928]
2. Mustafi D, Engel AH, Palczewski K. Structure of Cone Photoreceptors. *Prog. Retinal Eye Res.* 2009; 28:289–302.
3. Filipek S, Stenkamp RE, Teller DC, Palczewski K. G protein-coupled receptor rhodopsin: A prospectus. *Annu. Rev. Physiol.* 2003; 65:851–879. [PubMed: 12471166]
4. Palczewski K. G protein-coupled receptor rhodopsin. *Annu. Rev. Biochem.* 2006; 75:743–767. [PubMed: 16756510]
5. Nathans J, Thomas D, Hogness DS. Molecular genetics of human color vision: the genes encoding blue, green, and red pigments. *Science.* 1986; 232:193–202. [PubMed: 2937147]
6. Fasick JI, Lee N, Oprian DD. Spectral tuning in the human blue cone pigment. *Biochemistry.* 1999; 38:11593–11596. [PubMed: 10512613]
7. Yau KW, Hardie RC. Phototransduction motifs and variations. *Cell.* 2009; 139:246–264. [PubMed: 19837030]

8. Luo DG, Xue T, Yau KW. How vision begins: an odyssey. *Proc. Natl. Acad. Sci. U. S. A.* 2008; 105:9855–9862. [PubMed: 18632568]
9. Stenkamp RE, Filipek S, Driessen CAGG, Teller DC, Palczewski K. Crystal structure of rhodopsin: A template for cone visual pigments and other G protein-coupled receptors. *Biochim. Biophys. Acta, Biomembr.* 2002; 1565:168–182.
10. Kochendoerfer GG, Wang Z, Oprian DD, Mathies RA. Resonance Raman Examination of the Wavelength Regulation Mechanism in Human Visual Pigments. *Biochemistry.* 1997; 36:6577–6587. [PubMed: 9184137]
11. Sakmar TP, Franke RR, Khorana HG. Glutamic acid-113 serves as the retinylidene Schiff base counterion in bovine rhodopsin. *Proc. Natl. Acad. Sci. U. S. A.* 1989; 86:8309–8313. [PubMed: 2573063]
12. Palczewski K, Kumasaka T, Hori T, Behnke CA, Motoshima H, Fox BA, Le Trong I, Teller DC, Okada T, Stenkamp RE, Yamamoto M, Miyano M. Crystal structure of rhodopsin: A G protein-coupled receptor. *Science.* 2000; 289:739–745. [PubMed: 10926528]
13. Sakmar TP. Redder Than Red. *Science.* 2012; 338:1299–1300. [PubMed: 23224543]
14. Hubbard R. The Thermal Stability of Rhodopsin and Opsin. *J. Gen. Physiol.* 1958; 42:259–280. [PubMed: 13587911]
15. Chun E, Thompson AA, Liu W, Roth CB, Griffith MT, Katritch V, Kunken J, Xu F, Cherezov V, Hanson MA, Stevens RC. Fusion partner toolchest for the stabilization and crystallization of G protein-coupled receptors. *Structure.* 2012; 20:967–976. [PubMed: 22681902]
16. Liu W, Chun E, Thompson AA, Chubukov P, Xu F, Katritch V, Han GW, Roth CB, Heitman LH, IJerman AP, Cherezov V, Stevens RC. Structural basis for allosteric regulation of GPCRs by sodium ions. *Science.* 2012; 337:232–236. [PubMed: 22798613]
17. Rosenbaum DM, Cherezov V, Hanson MA, Rasmussen SG, Thian FS, Kobilka TS, Choi HJ, Yao XJ, Weis WI, Stevens RC, Kobilka BK. GPCR engineering yields high-resolution structural insights into beta2-adrenergic receptor function. *Science.* 2007; 318:1266–1273. [PubMed: 17962519]
18. Park SH, Das BB, Casagrande F, Tian Y, Nothnagel HJ, Chu M, Kiefer H, Maier K, De Angelis AA, Marassi FM, Opella SJ. Structure of the chemokine receptor CXCR1 in phospholipid bilayers. *Nature.* 2012; 491:779–783. [PubMed: 23086146]
19. Yin J, Mobarec JC, Kolb P, Rosenbaum DM. Crystal structure of the human OX2 orexin receptor bound to the insomnia drug suvorexant. *Nature.* 2015; 519:247–250. [PubMed: 25533960]
20. West GM, Chien EY, Katritch V, Gatchalian J, Chalmers MJ, Stevens RC, Griffin PR. Ligand-dependent perturbation of the conformational ensemble for the GPCR beta2 adrenergic receptor revealed by HDX. *Structure.* 2011; 19:1424–1432. [PubMed: 21889352]
21. Warne T, Serrano-Vega MJ, Baker JG, Moukhametzianov R, Edwards PC, Henderson R, Leslie AG, Tate CG, Schertler GF. Structure of a beta1-adrenergic G-protein-coupled receptor. *Nature.* 2008; 454:486–491. [PubMed: 18594507]
22. Crabb JW, Cehen Y, Goldflam S, Intres R, West KA, Hulmes JD, Kapron JT, Luck LA, Carlson A, Bok D, Horwitz J. Structural and functional characterization of recombinant human cellular retinaldehyde-binding protein. *Protein Sci.* 1998; 7:746–757. [PubMed: 9541407]
23. Medina R, Perdomo D, Bubis J. The hydrodynamic properties of dark- and light-activated states of *n*-dodecyl beta-d-maltoside-solubilized bovine rhodopsin support the dimeric structure of both conformations. *J. Biol. Chem.* 2004; 279:39565–39573. [PubMed: 15258159]
24. Fotiadis D, Liang Y, Filipek S, Saperstein DA, Engel A, Palczewski K. The G protein-coupled receptor rhodopsin in the native membrane. *FEBS Lett.* 2004; 564:281–288. [PubMed: 15111110]
25. Mayhew SG, Massey V. Purification and Characterization of Flavodoxin from *Peptostreptococcus elsdenii*. *J. Biol. Chem.* 1969; 244:794–802. [PubMed: 4976788]
26. Liu T, Jenwitheesuk E, Teller DC, Samudrala R. Structural insights into the cellular retinaldehyde-binding protein (CRALBP). *Proteins: Structure, Funct., Genet.* 2005; 61:412–422. [PubMed: 16121400]
27. Bolze CS, Helbling RE, Owen RL, Pearson AR, Pompidor G, Dworkowski F, Fuchs MR, Furrer J, Golczak M, Palczewski K, Cascella M, Stocker A. Human Cellular Retinaldehyde-Binding Protein

- Has Secondary Thermal 9-cis-Retinal Isomerase Activity. *J. Am. Chem. Soc.* 2014; 136:137–146. [PubMed: 24328211]
28. Okada T, Palczewski K. Crystal structure of rhodopsin: Implications for vision and beyond. *Curr. Opin. Struct. Biol.* 2001; 11:420–426. [PubMed: 11495733]
29. Schneider EH, Seifert R. Sf9 cells: A versatile model system to investigate the pharmacological properties of G protein-coupled receptors. *Pharmacol. Ther.* 2010; 128:387–418. [PubMed: 20705094]
30. Cherezov V, Rosenbaum DM, Hanson MA, Rasmussen SGF, Thian FS, Kobilka TS, Choi H-J, Kuhn P, Weis WI, Kobilka BK, Stevens RC. High Resolution Crystal Structure of an Engineered Human $\beta(2)$ -Adrenergic G protein-Coupled Receptor. *Science (Washington, DC, U.S.)*. 2007; 318:1258–1265.
31. Jaakola V-P, Griffith MT, Hanson MA, Cherezov V, Chien EYT, Lane JR, Ijzerman AP, Stevens RC. The 2.6 Å Crystal Structure of a Human A(2A) Adenosine Receptor Bound to an Antagonist. *Science (Washington, DC, U.S.)*. 2008; 322:1211–1217.
32. Chien EYT, Liu W, Zhao Q, Katritch V, Han GW, Hanson MA, Shi L, Newman AH, Javitch JA, Cherezov V, Stevens RC. Structure of the human dopamine D3 receptor in complex with a D2/D3 selective antagonist. *Science (Washington, DC, U.S.)*. 2010; 330:1091–1095.
33. Wu B, Chien EYT, Mol CD, Fenalti G, Liu W, Katritch V, Abagyan R, Brooun A, Wells P, Bi FC, Hamel DJ, Kuhn P, Handel TM, Cherezov V, Stevens RC. Structures of the CXCR4 chemokine receptor in complex with small molecule and cyclic peptide antagonists. *Science (Washington, DC, U.S.)*. 2010; 330:1066–1071.
34. Chun E, Thompson AA, Liu W, Roth CB, Griffith MT, Katritch V, Kunken J, Xu F, Cherezov V, Hanson MA, Stevens RC. Fusion Partner Toolchest for the Stabilization and Crystallization of G Protein-Coupled Receptors. *Structure (Oxford, U.K.)*. 2012; 20:967–976.
35. Rath A, Glibowicka M, Nadeau VG, Chen G, Deber CM. Detergent binding explains anomalous SDS-PAGE migration of membrane proteins. *Proc. Natl. Acad. Sci. U.S.A.* 2009; 106:1760–1765. [PubMed: 19181854]
36. Chae PS, Rasmussen SGF, Rana RR, Gotfryd K, Chandra R, Goren MA, Kruse AC, Nurva S, Loland CJ, Pierre Y, Drew D, Popot J-L, Picot D, Fox BG, Guan L, Gether U, Byrne B, Kobilka B, Gellman SH. Maltoseneopentyl glycol (MNG) amphiphiles for solubilization, stabilization and crystallization of membrane proteins. *Nat. Methods.* 2010; 7:1003–1008. [PubMed: 21037590]
37. Vissers PM, Bovee-Geurts PH, Portier MD, Klaassen CH, Degrip WJ. Large-scale production and purification of the human green cone pigment: Characterization of late photo-intermediates. *Biochem. J.* 1998; 330:1201–1208. [PubMed: 9494086]

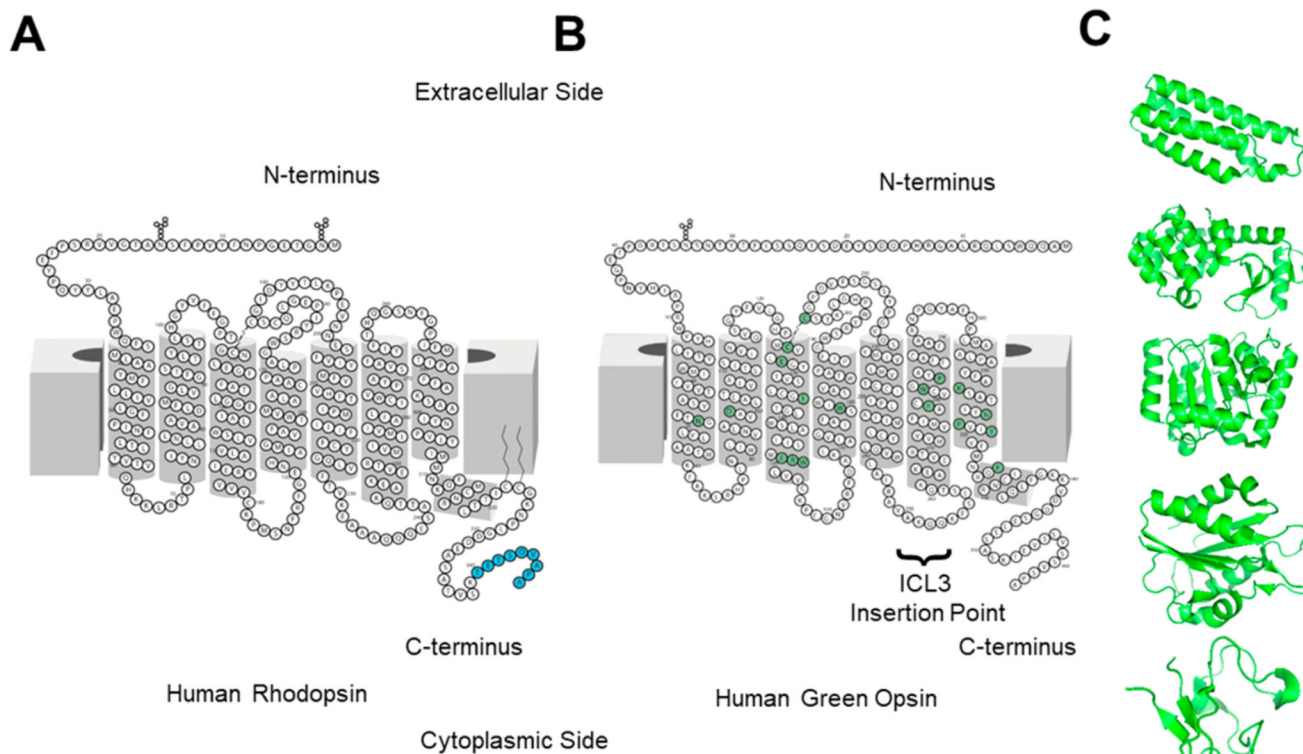


Figure 1.

2D Models comparing (A) Human Rhodopsin and (B) Human Green Opsin. Anti-Rho "1D4" epitope residues are colored in blue for panel (A). Key residues in panel (B) are shown in green highlighted circles.⁹ Known glycosylation sites are denoted by small branched chains on the extracellular side of these proteins. Palmitoyl groups of Rho are also shown at Cys residues 322 and 323 denoted by a fatty acid carbon chain. (C) Structures of the five domains selected for fusion into the third intracellular loop of human green opsin (shown in B). The five domains are Cytochrome *b*₆₃₀RIL (PDB ID 1M6T), T4 lysozyme (PDB ID 2LZM), the C-terminal domain of glycogen synthase (PDB ID 2BFW), flavodoxin (PDB ID 1I1O), and rubredoxin (PDB ID 1FHM).

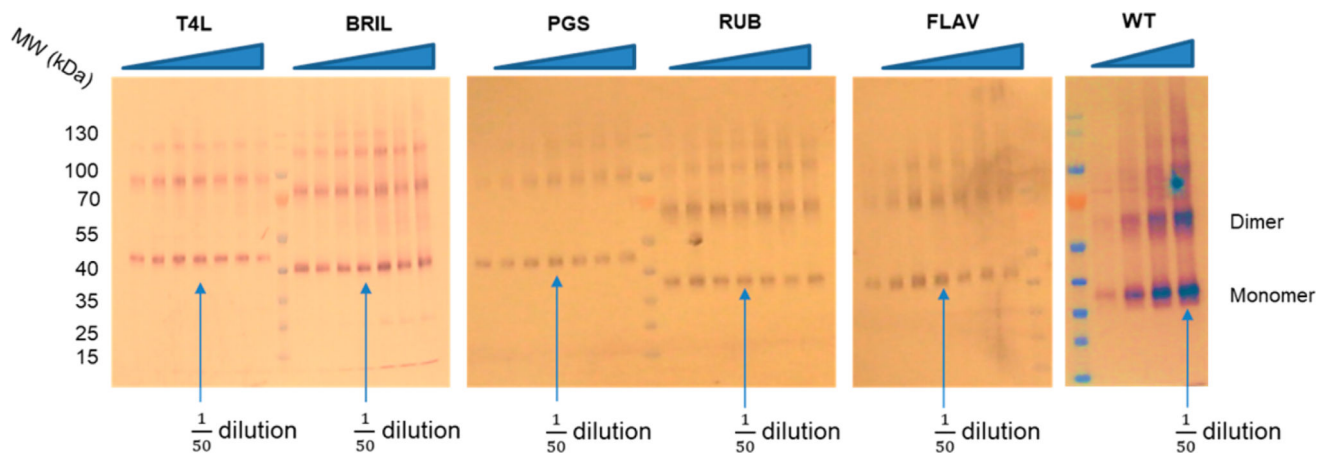


Figure 2.

Expression by virus titration. P3 stage virus was used to infect the same amount of Sf9 cells. For each construct, the virus was added in increasing (doubled) amounts from left to right lanes from a 1:400 dilution to a 1:6.25 dilution factor. All samples were harvested on day 2 and subjected to SDS-PAGE before their transfer to a PVDF membrane for detection with 1D4 antibody. The quantity of P3 stage virus used for infection appears to maximize opsin expression at an average dilution of 1:50. The apparent mass of each construct was as follows WT 38 kDa (40.3 kDa expected), T4L 44 kDa (56.5 kDa expected), BRIL 41 kDa (50.5 kDa expected), PGS 46 kDa (60.5 kDa expected), RUB 39 kDa (44.5 kDa expected), and FLAV 40 kDa (54.5 kDa expected).

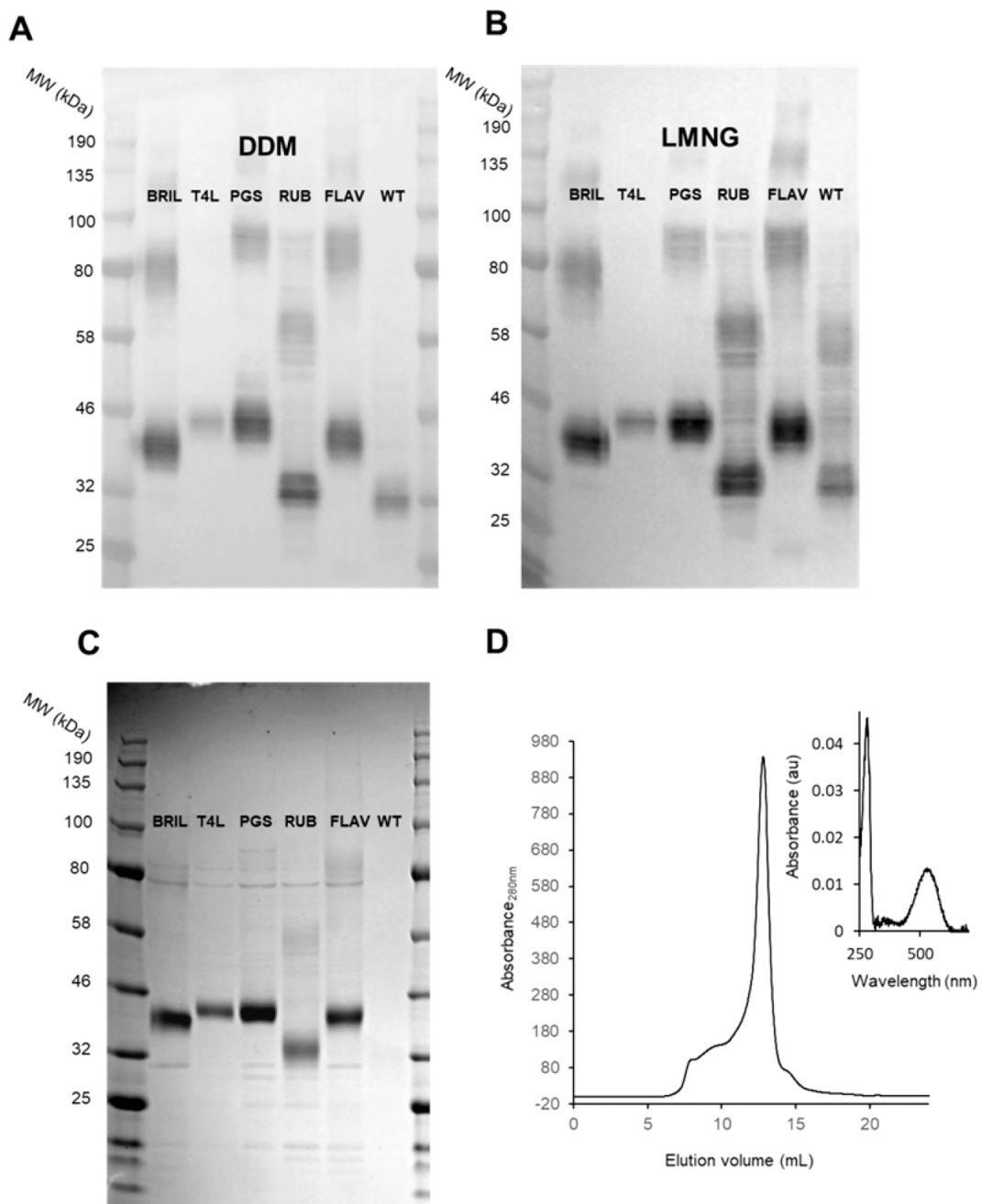


Figure 3.

1D4 immunoblot of the six green opsin constructs solubilized in either (A) DDM or (B) LMNG. (C) Coomassie-stained SDS-PAGE of the six green opsin constructs purified in DDM. (D) Gel filtration profile of the green-PGS opsin construct. The column used was a Superdex 200, and the running buffer was 10 mM HEPES, pH 7.0, 0.1 M NaCl, and 0.2 mM LMNG. The sample injected consisted of 0.5 mL of 2.7 mg/mL green-PGS opsin construct previously purified by 1D4 immunochromatography. Inset shows the UV-Vis absorption spectrum of the peak fraction (diluted 30 times in running buffer).

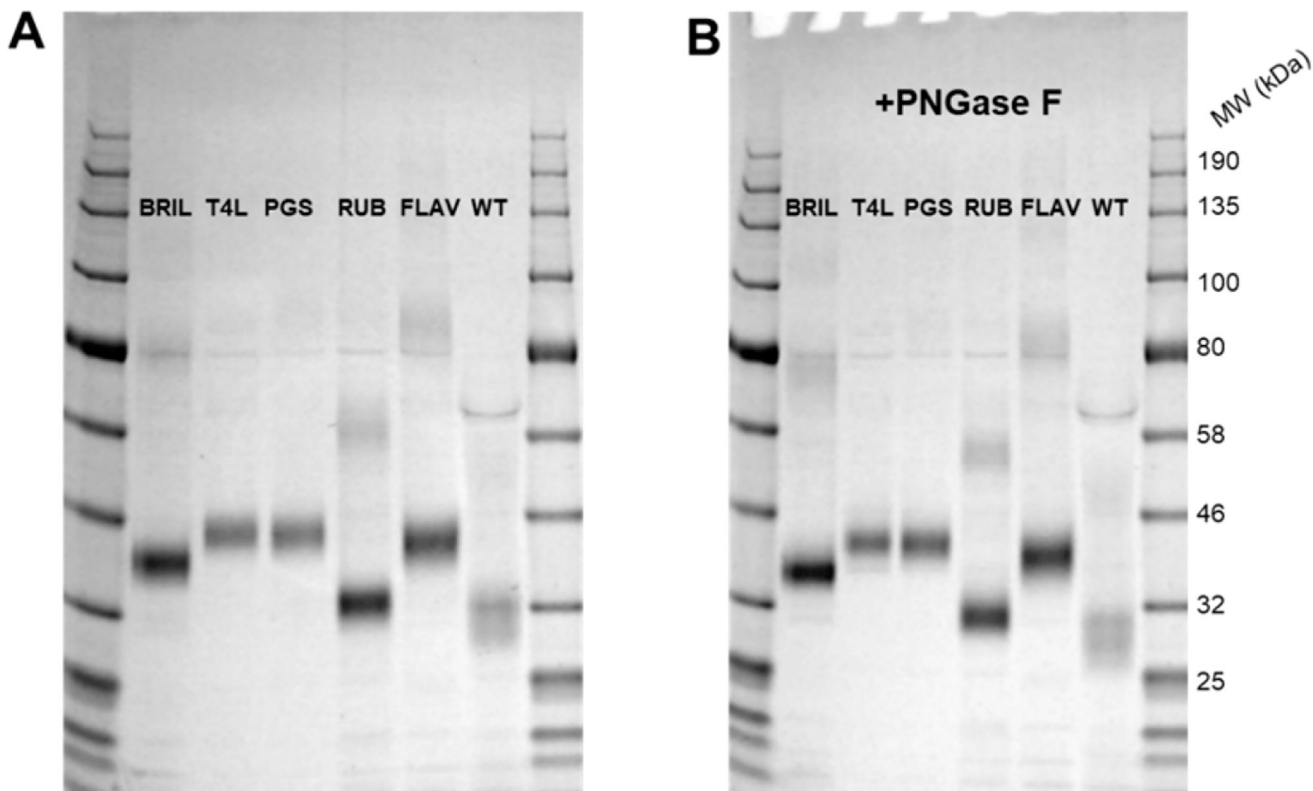


Figure 4.

(A) Silver-stained SDS-PAGE of the six green opsin constructs purified in LMNG. For each construct, 10 ng of purified green opsin was loaded per lane. (B) Samples were treated with PNGase F and silver-stained. A 2–3 kDa mass shift indicates that the green pigment is deglycosylated and correlates with ~1 glycosylation site, as indicated by the sequence of the WT-green opsin (Figure 1).

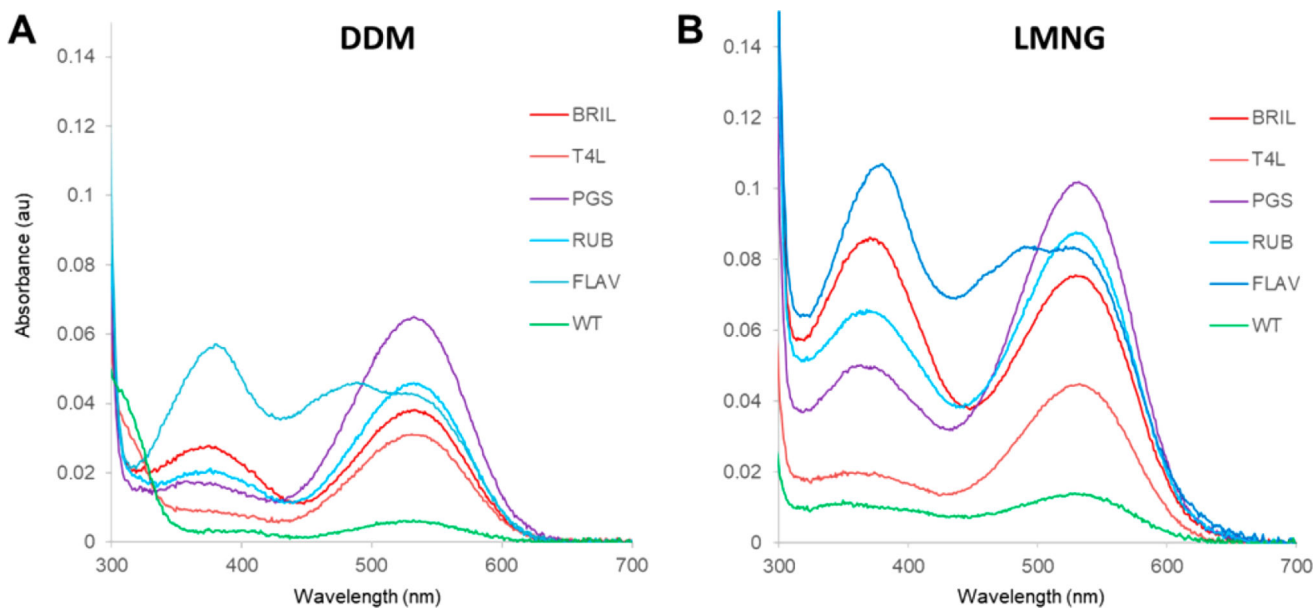
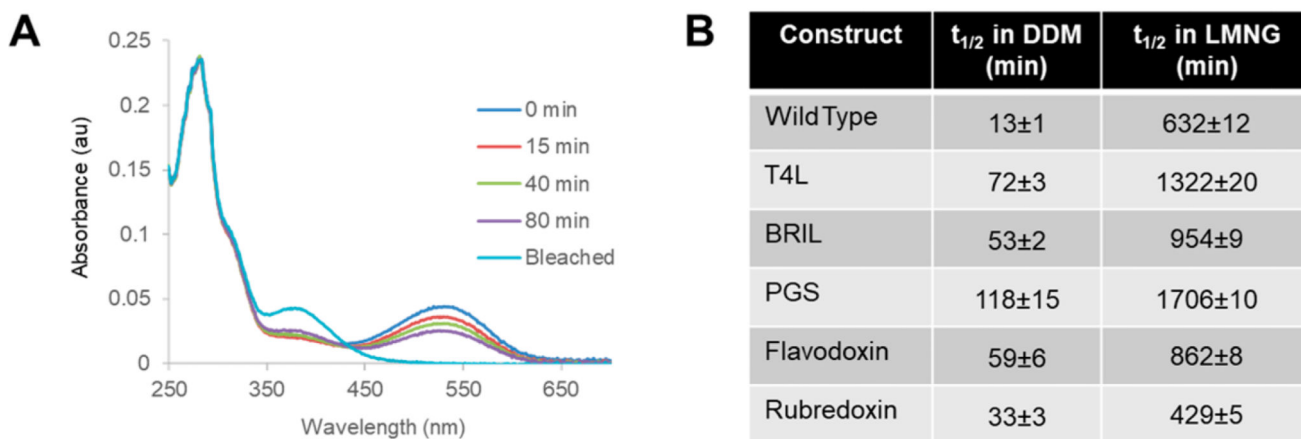


Figure 5. Visible absorption spectra of the six green opsin constructs purified in either (A) DDM or (B) LMNG. All constructs appear to have a native green pigment active site as their absorbance maxima coincides with the WT opsin absorbance at 530 nm. Constructs purified in DDM show ~50% less native opsin eluted from the 1D4-Sepharose due to ~50% less absorbance at 530 nm, indicating preferential solubilization into LMNG micelles.

**Figure 6.**

(A) Thermal decay of the active site chromophore in PGS Green Cone Pigment fusion protein in DDM at 30 °C. Here, k_{obs} was determined by plotting the decay at 530 nm over time and its value was subsequently employed to calculate the apparent half-life of each construct. (B) Apparent half-life at 30 °C of each construct purified either in DDM or LMNG.

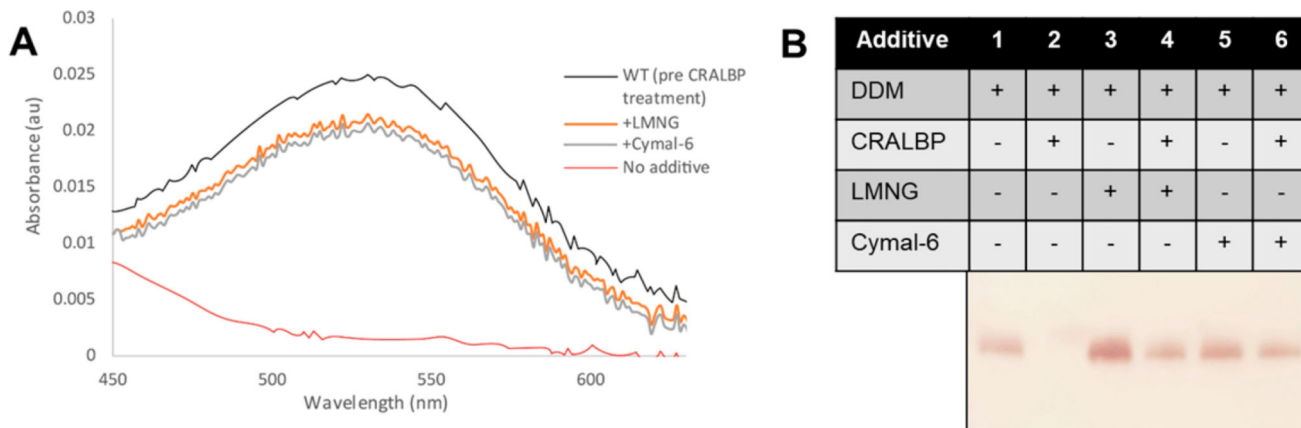


Figure 7.

(A) CRALBP competition assay reveals that, following incubation with WT pigment purified in DDM, the chromophore peak disappears at 530 nm. Incubation of WT pigment with LMNG or Cymal-6 preserves the chromophore peak. (B) Samples tested in panel (A) were subjected to immunoblotting using 1D4-antibody. Disappearance of the WT-pigment was confirmed by the loss of the corresponding protein band while samples incubated with LMNG or Cymal-6 were preserved, maintaining the chromophore peak at 530 nm.